

*MAT_162
*MAT_COMPOSITE_MSC_DMG

A PROGRESSIVE COMPOSITE DAMAGE MODEL FOR UNIDIRECTIONAL AND WOVEN FABRIC COMPOSITES

**UD-CCM Updates on MAT162 USER MANUAL
Version 14C-2014**

Materials Sciences Corporation
&
University of Delaware Center for Composite Materials

December 2014

Technical Support
Dr. Bazle Z. (Gama) Haque
E-mail: gama@udel.edu, Tel: (302) 690-4741
© University of Delaware Center for Composite Materials. All Rights Reserved.

***MAT_COMPOSITE_MSC_{OPTION}**

Available options include:

<BLANK>

DMG

These are Material Types 161 and 162. These material types may be used to model the progressive failure in composite materials consisting of unidirectional and woven fabric layers subjected to high strain-rate and high pressure loading conditions. The progressive layers failure criteria have been established by adopting the methodology developed by Hashin [1980] with a generalization to include the effect of highly constrained pressure on composite failure. These failure models can be used to effectively simulate fiber failure, matrix damage, and delamination behavior under all conditions – opening, closure, and sliding of failure surfaces. The model with DMG option (material 162) is a generalization of the basic layer failure model of Material 161 by adopting the damage mechanics approach [Matzenmiller et al., 1995] for characterizing the softening behavior after damage initiation. These models require an additional license from Materials Sciences Corporation, which developed and supports these models in collaboration with University of Delaware Center for Composite Materials (UD-CCM).

Card 1	1	2	3	4	5	6	7	8
Variable	MID	RO	EA	EB	EC	PRBA	PRCA	PRCB
Type	A8	F	F	F	F	F	F	F

Card 2	1	2	3	4	5	6	7	8
Variable	GAB	GBC	GCA	AOPT	MACF			
Type	F	F	F	F	I			

Card 3	1	2	3	4	5	6	7	8
Variable	XP	YP	ZP	A1	A2	A3		
Type	F	F	F	F	F	F		

Card 4	1	2	3	4	5	6	7	8
Variable	V1	V2	V3	D1	D2	D3	BETA	
Type	F	F	F	F	F	F	F	

Card 5	1	2	3	4	5	6	7	8
Variable	SAT	SAC	SBT	SBC	SCT	SFC	SFS	S_AB
Type	F	F	F	F	F	F	F	F

Card 6	1	2	3	4	5	6	7	8
Variable	S_BC	S_CA	SFFC	AMODEL	PHIC	E_LIMT	S_DELM	
Type	F	F	F	F	F	F	F	

Card 7	1	2	3	4	5	6	7	8
Variable	OMGMX	ECRSH	EEXPV	CERATE1	AM1			
Type	F	F	F	F	F			

Define the following card if and only if the option DMG is specified.

Card 8	1	2	3	4	5	6	7	8
Variable	AM2	AM3	AM4	CERATE2	CERATE3	CERATE4		
Type	F	F	F	F	F	F		

VARIABLE**DESCRIPTION**

MID	Material identification. A unique number or label not exceeding 8 characters must be specified.
RO	Mass density
EA	E_a , Young's modulus - longitudinal direction [♥]
EB	E_b , Young's modulus - transverse direction [♥]
EC	E_c , Young's modulus – through thickness direction [♥]
PRBA	ν_{ba} , Poisson's ratio ba
PRCA	ν_{ca} , Poisson's ratio ca
PRCB	ν_{cb} , Poisson's ratio cb
GAB	G_{ab} , shear modulus ab
GBC	G_{bc} , shear modulus bc
GCA	G_{ca} , shear modulus ca

[♥] LS-DYNA[®] notations a, b, & c have the same meaning as for orthotropic material axes notations 1, 2, & 3.

<u>VARIABLE</u>	<u>DESCRIPTION</u>
AOPT	<p>Material axes option, see Figure 2.1. (in KEYWORD Manual)</p> <p>EQ.0.0: locally orthotropic with material axes determined by element nodes as shown in Figure 2.1. Nodes 1, 2, and 4 of an element are identical to the Nodes used for the definition of a coordinate system by *DEFINE_COORDINATE_NODES.</p> <p>EQ.1.0: locally orthotropic with material axes determined by a point in space and the global location of the element center, this is the a-direction.</p> <p>EQ.2.0: globally orthotropic with material axes determined by vectors defined below, as with *DEFINE_COORDINATE_VECTOR.</p> <p>LT.0.0: the absolute value of AOPT is a coordinate system ID number (CID on *DEFINE_COORDINATE_NODES, *DEFINE_COORDINATE_SYSTEM or *DEFINE_COORDINATE_VECTOR). Available in R3 version of 971 and later.</p>
MACF	<p>Material axes change flag:</p> <p>EQ.1: No change, default,</p> <p>EQ.2: switch material axes a & b,</p> <p>EQ.3: switch material axes a & c,</p> <p>EQ.4: switch material axes b & c.</p>
XP YP ZP	Define coordinates of point p for AOPT = 1.
A1 A2 A3	Define components of vector a for AOPT = 2.
V1 V2 V3	Define components of vector v for AOPT = 3.
D1 D2 D3	Define components of vector d for AOPT = 2.
BETA	Layer in-plane rotational angle in degrees.
SAT	Longitudinal tensile strength, S_{aT}
SAC	Longitudinal compressive strength, S_{aC}
SBT	Transverse tensile strength, S_{bT}
SBC	Transverse compressive strength, S_{bC}
SCT	Through thickness tensile strength, S_{cT}
SFC	Crush strength, S_{FC}
SFS	Fiber mode shear strength, S_{FS}

<u>VARIABLE</u>	<u>DESCRIPTION</u>
S_AB [♦]	Matrix mode shear strength, ab plane, see below, S_{ab}
S_BC [♦]	Matrix mode shear strength, bc plane, see below, S_{bc}
S_CA [♦]	Matrix mode shear strength, ca plane, see below, S_{ca}
SFFC	Scale factor for residual compressive strength, S_{FFC}
AMODEL	Material models: EQ.1: Unidirectional lamina model EQ.2: Fabric lamina model
PHIC	Coulomb friction angle for matrix and delamination failure, $\varphi < 90^\circ$
S_DELM	Scale factor for delamination criterion, S
OMGMX	Limit damage parameter for elastic modulus reduction, ϖ_{\max}
E_LIMT	Element eroding axial strain
ECRSH	Limit compressive relative volume for element eroding
EEXPN	Limit expansive relative volume for element eroding
CERATE1	Coefficient for strain rate dependent strength properties, C_{rate1}
CERATE2	Coefficient for strain rate dependent axial moduli, C_{rate2}
CERATE3	Coefficient for strain rate dependent shear moduli, C_{rate3}
CERATE4	Coefficient for strain rate dependent transverse moduli, C_{rate4}
AM1	Coefficient for strain softening property for fiber damage in a direction, m_1
AM2	Coefficient for strain softening property for transverse compressive matrix failure mode in b direction (unidirectional) or for fiber damage mode in b direction (fabric), m_2
AM3	Coefficient for strain softening property for fiber crush and punch shear damage, m_3
AM4	Coefficient for strain softening property for matrix failure and delamination damage, m_4

[♦] LS-DYNA KEYWORD manual presents these parameters as: SAB, SBC, & SCA. Since SBC is also used to define the “transverse compressive strength,” we have used S_xx to represent shear strength in xx plane.

Figure 2.1. from the KEYWORD Manual of LS-DYNA® is reproduced here for the convenience of the MAT162 users.

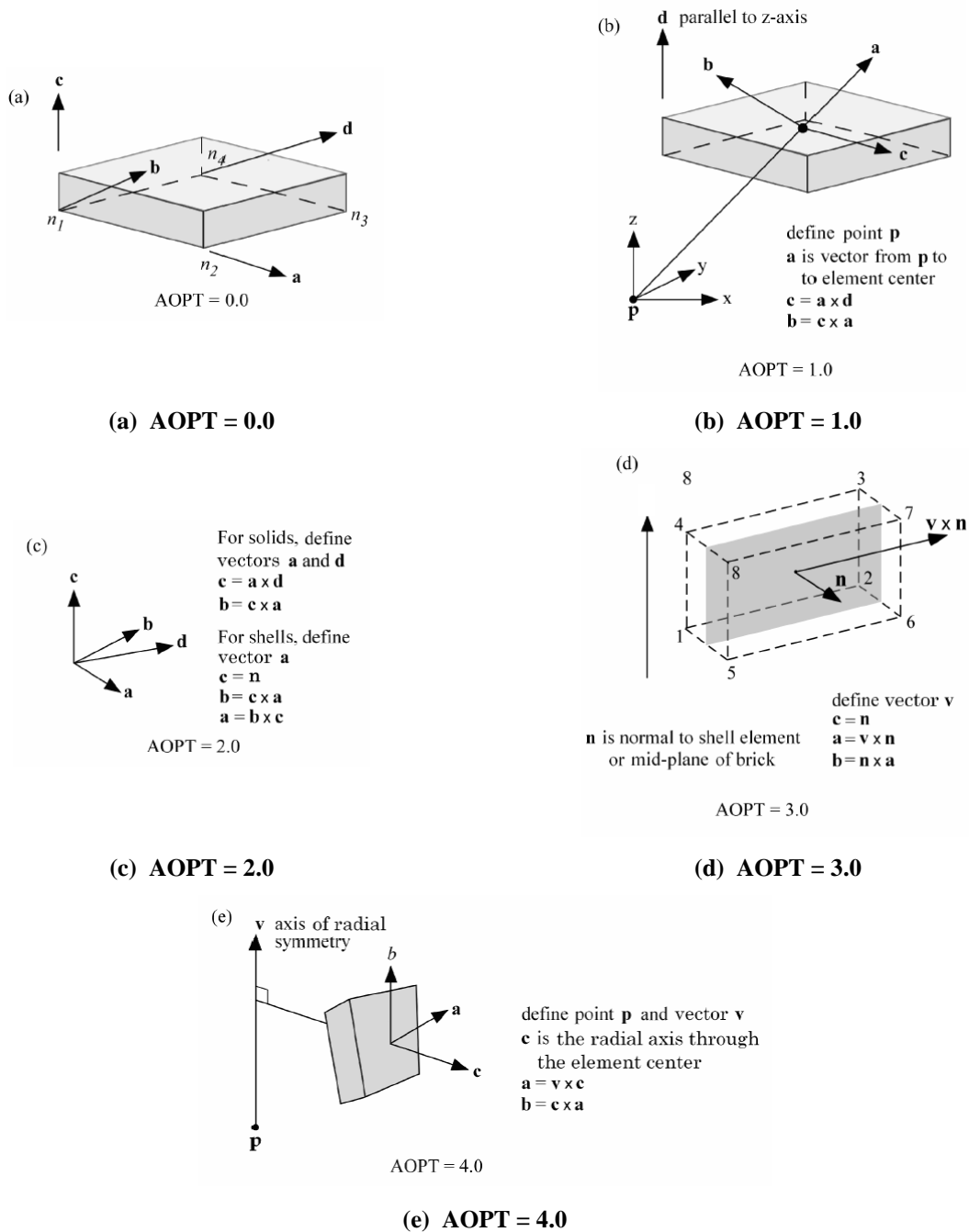


Figure 2.1. Options for determining principal material axes: (a) AOPT = 0.0, (b) AOPT = 1.0 for brick elements, (c) AOPT = 2.0, (d) AOPT = 3.0, and (e) AOPT=4.0 for brick elements.

Figure 1: Material Axes Definition presented in the LS-DYNA KEYWORD Manual (OLDER VERSIONS)

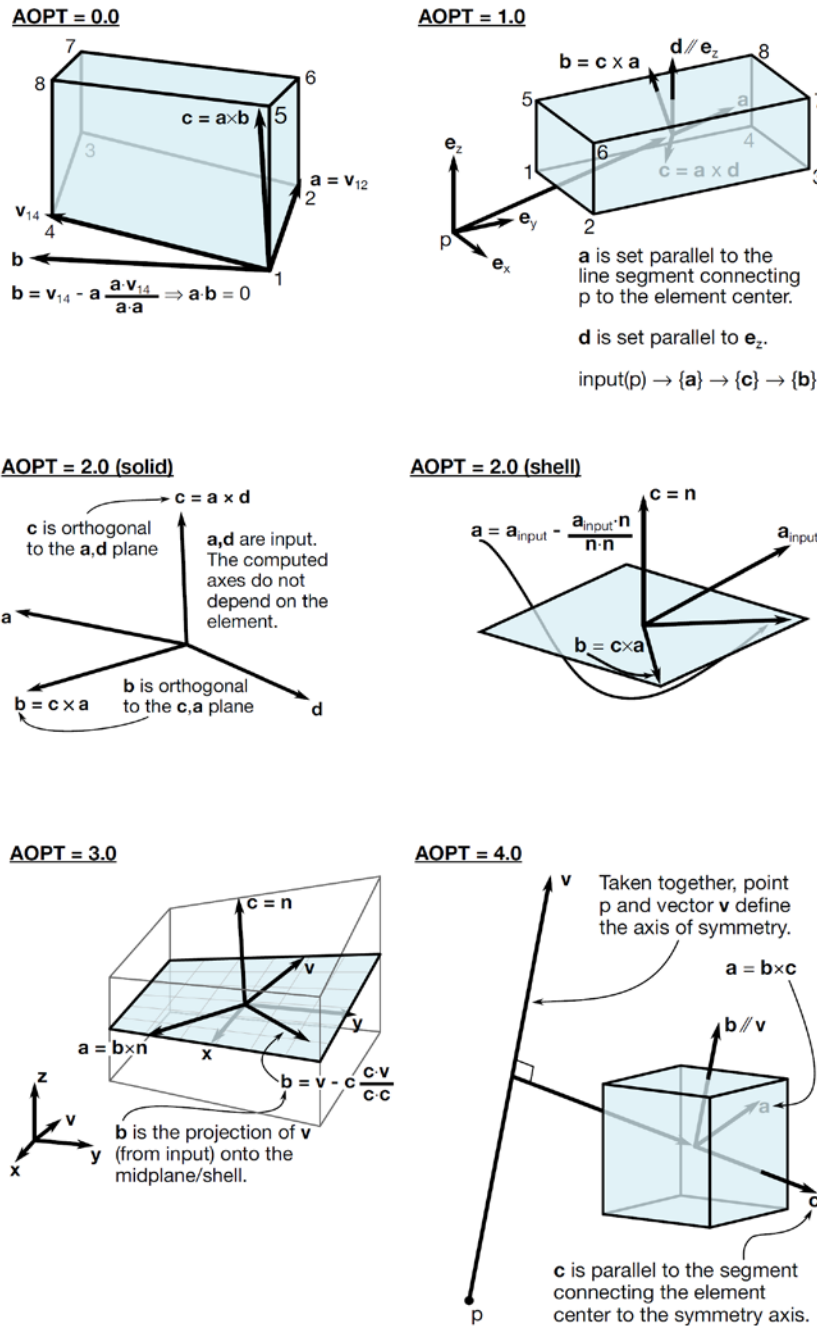


Figure 1 (Continued): Material Axes Definition presented in the LS-DYNA Manuals (NEW VERSIONS, May 2014)

MATERIAL MODELS

Failure models based on the 3D stresses/strains in a composite lamina with improved progressive failure modeling capability are established for a unidirectional and for a fabric composite lamina. **While the LS-DYNA KEYWORD manual presents the stress based formulations, this manual presents the strain based formulations.** These models can be used to effectively simulate the fiber failure, matrix failure, and delamination behavior of composites under high strain-rate and high pressure ballistic impact conditions.

The unidirectional and fabric lamina failure criteria and the associated property degradation models are described as follows. All the failure criteria are expressed in terms of stress components based on ply level strains $(\varepsilon_1, \varepsilon_2, \varepsilon_3, \varepsilon_{12}, \varepsilon_{23}, \varepsilon_{31}) = (\varepsilon_a, \varepsilon_b, \varepsilon_c, \varepsilon_{ab}, \varepsilon_{bc}, \varepsilon_{ca})$. The associated elastic moduli are $(E_1, E_2, E_3, G_{12}, G_{23}, G_{31}) = (E_a, E_b, E_c, G_{ab}, G_{bc}, G_{ca})$. Note that for the unidirectional model, a, b, and c denote the fiber, in-plane transverse and out-of-plane or through-thickness directions, respectively; while for the fabric model, a, b, and c denote the in-plane fill, in-plane warp and out-of-plane or through-thickness directions, respectively.

UNIDIRECTIONAL LAMINA DAMAGE MODEL

Fiber Mode Failures

The fiber failure criteria of Hashin [1980] for a unidirectional layer are generalized to characterize the fiber damage in terms of strain components for a unidirectional layer. Three damage functions are used for fiber failure, one in tension/shear, one in compression, and another one in crush under pressure. They are chosen in terms of quadratic strain forms as follows:

TENSION-SHEAR FIBER MODE: MODE 1u

$$f_1 - r_1^2 = \left(\frac{E_a \langle \varepsilon_a \rangle}{S_{aT}} \right)^2 + \left(\frac{G_{ab}^2 \varepsilon_{ab}^2 + G_{ca}^2 \varepsilon_{ca}^2}{S_{FS}^2} \right) - r_1^2 = 0 \quad (1)$$

COMPRESSION FIBER MODE: MODE 2u

$$f_2 - r_2^2 = \left(\frac{E_a \langle \varepsilon'_a \rangle}{S_{aC}} \right)^2 - r_2^2 = 0, \rightarrow \varepsilon'_a = -\varepsilon_a - \frac{\langle -E_c \varepsilon_c - E_b \varepsilon_b \rangle}{2E_a} \quad (2)$$

CRUSH MODE: MODE 3u

$$f_3 - r_3^2 = \left(\frac{E_c \langle -\varepsilon_c \rangle}{S_{FC}} \right)^2 - r_3^2 = 0 \quad (3)$$

where $\langle \rangle$ are Macaulay brackets, S_{aT} and S_{aC} are the tensile and compressive strengths in the fiber direction, and S_{FS} and S_{FC} are the layer strengths associated with the fiber shear and crush failure, respectively. The damage thresholds, r_j , $j = 1, 2, 3$, have the initial values equal to 1 before the damage initiated, and are updated due to damage accumulation in the associated damage modes.

Matrix Mode Failures

Matrix mode failures must occur without fiber failure, and hence they will be on planes parallel to fibers. Two matrix damage functions are chosen for the failure plane perpendicular and parallel to the layering planes. They have the forms:

TRANSVERSE COMPRESSIVE MATRIX MODE: MODE 4u

$$f_4 - r_4^2 = \left(\frac{E_b \langle -\varepsilon_b \rangle}{S_{bC}} \right)^2 - r_4^2 = 0 \quad (4)$$

PERPENDICULAR MATRIX MODE: MODE 5u

$$f_5 - r_5^2 = \left(\frac{E_b \langle \varepsilon_b \rangle}{S_{bT}} \right)^2 + \left(\frac{G_{bc} \varepsilon_{bc}}{S_{bc0} + S_{SRB}} \right)^2 + \left(\frac{G_{ab} \varepsilon_{ab}}{S_{ab0} + S_{SRB}} \right)^2 - r_5^2 = 0 \quad (5)$$

PARALLEL MATRIX MODE (DELAMINATION): MODE 6u

$$f_6 - r_6^2 = S^2 \left\{ \left(\frac{E_c \langle \varepsilon_c \rangle}{S_{cT}} \right)^2 + \left(\frac{G_{bc} \varepsilon_{bc}}{S_{bc0} + S_{SRC}} \right)^2 + \left(\frac{G_{ca} \varepsilon_{ca}}{S_{ca0} + S_{SRC}} \right)^2 \right\} - r_6^2 = 0 \quad (6)$$

where S_{bT} and S_{cT} are the transverse tensile strengths of the corresponding tensile modes ($\varepsilon_b > 0$ or $\varepsilon_c > 0$); and S_{ab0} , S_{bc0} , & S_{ca0} are the quasi-static shear strength values. Under compressive transverse strain, $\varepsilon_b < 0$ or $\varepsilon_c < 0$, the damaged surface is considered to be “closed”, and the shear strengths are assumed to depend on the compressive normal strains based on the Mohr-Coulomb theory, i.e.:

$$\begin{aligned} S_{SRB} &= E_b \tan(\varphi) \langle -\varepsilon_b \rangle \\ S_{SRC} &= E_c \tan(\varphi) \langle -\varepsilon_c \rangle \end{aligned} \quad (7)$$

where φ is a material constant as $\tan(\varphi)$ is similar to the coefficient of friction. The damage thresholds r_j , $j = 4, 5, 6$, have the initial values equal to 1 before the damage initiated, and are updated due to damage accumulation of the associated damage modes.

Failure predicted by the criterion of f_4 and f_5 can be referred to as transverse matrix failure, while the matrix failure predicted by f_6 , which is parallel to the layer, can be referred as the delamination mode when it occurs within the elements that are adjacent to the ply interface. Note that a scale factor S is introduced to provide better correlation of delamination area with experiments. The scale factor S can be determined by fitting the analytical prediction to experimental data for the delamination area.

FABRIC LAMINA DAMAGE MODEL

Fiber Mode Failures

The fiber failure criteria of Hashin [1980] for a unidirectional layer are generalized to characterize the fiber damage in terms of strain components for a plain weave layer. The fill and warp fiber tensile/shear damage are given by the quadratic interaction between the associated axial and through the thickness shear strains, i.e.:

TENSION-SHEAR FIBER MODES: MODE 1f & 2f

$$\begin{aligned} f_7 - r_7^2 &= \left(\frac{E_a \langle \varepsilon_a \rangle}{S_{aT}} \right)^2 + \left(\frac{G_{ca} \varepsilon_{ca}}{S_{aFS}} \right)^2 - r_7^2 = 0 \\ f_8 - r_8^2 &= \left(\frac{E_b \langle \varepsilon_b \rangle}{S_{bT}} \right)^2 + \left(\frac{G_{bc} \varepsilon_{bc}}{S_{bFS}} \right)^2 - r_8^2 = 0 \end{aligned} \quad (8)$$

where S_{aT} and S_{bT} are the axial tensile strengths in the fill and warp directions, respectively, and S_{aFS} and S_{bFS} are the lamina shear strengths due to fiber shear failure in the fill and warp directions. These failure criteria are applicable when the associated ε_a or ε_b is positive. The damage thresholds r_7 and r_8 are equal to 1 without damage. It is assumed $S_{aFS} = S_{FS}$, and $S_{bFS} = S_{FS} \times S_{bT} / S_{aT}$.

COMPRESSION FIBER MODES: MODE 3f & 4f

When ε_a or ε_b is compressive, it is assumed that the in-plane compressive damage in the fill and warp directions are given by the maximum strain criterion, i.e.:

$$\begin{aligned} f_9 - r_9^2 &= \left(\frac{E_a \langle \varepsilon'_a \rangle}{S_{aC}} \right)^2 - r_9^2 = 0 \rightarrow \varepsilon'_a = -\varepsilon_a - \langle -\varepsilon_c \rangle \frac{E_c}{E_a} \\ f_{10} - r_{10}^2 &= \left(\frac{E_b \langle \varepsilon'_b \rangle}{S_{bC}} \right)^2 - r_{10}^2 = 0 \rightarrow \varepsilon'_b = -\varepsilon_b - \langle -\varepsilon_c \rangle \frac{E_c}{E_b} \end{aligned} \quad (9)$$

where S_{aC} and S_{bC} are the axial compressive strengths in the fill and warp directions, respectively, and r_9 and r_{10} are the corresponding damage thresholds. Note that the effect of through the thickness compressive strain on the in-plane compressive damage is taken into account in the above two equations.

CRUSH MODE: MODE 5f

When a composite material is subjected to transverse impact by a projectile, high compressive stresses will generally occur in the impact area with high shear stresses in the surrounding area between the projectile and the target material. While the fiber shear punch damage due to the high shear stresses can be accounted for by equation (1), the crush damage due to the high through the thickness compressive pressure is modeled using the following criterion:

$$f_{11} - r_{11}^2 = \left(\frac{E_c \langle -\varepsilon_c \rangle}{S_{FC}} \right)^2 - r_{11}^2 = 0 \quad (10)$$

where S_{FC} is the fiber crush strengths and r_{11} is the associated damage threshold.

Matrix Mode Failures

IN-PLANE MATRIX MODE: MODE 6f

A plain weave layer can be damaged under in-plane shear stressing without occurrence of fiber breakage. This in-plane matrix damage mode is given by:

$$f_{12} - r_{12}^2 = \left(\frac{G_{ab} \varepsilon_{ab}}{S_{ab}} \right)^2 - r_{12}^2 = 0 \quad (11)$$

where S_{ab} is the layer shear strength due to matrix shear failure and r_{12} is the damage threshold.

PARALLEL MATRIX MODE (DELAMINATION): MODE 7f

Another failure mode, which is due to the quadratic interaction between the transverse strains, is expected to be mainly a matrix failure. This through the thickness matrix failure criterion is assumed to have the following form:

$$f_{13} - r_{13}^2 = S^2 \left\{ \left(\frac{E_c \langle \varepsilon_c \rangle}{S_{cT}} \right)^2 + \left(\frac{G_{bc} \varepsilon_{bc}}{S_{bc0} + S_{SRC}} \right)^2 + \left(\frac{G_{ca} \varepsilon_{ca}}{S_{ca0} + S_{SRC}} \right)^2 \right\} - r_{13}^2 = 0 \quad (12)$$

where r_{13} is the damage threshold, S_{cT} is the through the thickness tensile strength for tensile ε_c , and S_{bc0} and S_{ca0} are the quasi-static shear strengths. The damage surface due to equation (12) is parallel to the composite layering plane. Under compressive through the thickness strain, $\varepsilon_c < 0$,

the damaged surface (delamination) is considered to be “closed”, and the shear strengths are assumed to depend on the compressive normal strain ε_c similar to the Mohr-Coulomb theory, i.e.:

$$S_{SRC} = E_c \tan(\varphi) \langle -\varepsilon_c \rangle \quad (13)$$

where φ is the Coulomb’s friction angle. When damage predicted by this criterion occurs within elements that are adjacent to the ply interface, the failure plane is expected to be parallel to the layering planes, and, thus, can be referred to as the delamination mode. Note that a scale factor S is introduced to provide better correlation of delamination area with experiments. The scale factor S can be determined by fitting the analytical prediction to experimental data for the delamination area.

DAMAGE PROGRESSION MODEL

A set of damage variables ϖ_i with $i = 1, \dots, 6$; are introduced to relate the onset and growth of damage to stiffness losses in the material. The compliance matrix $[S]$ is related to the damage variables as (Matzenmiller, et al., 1995):

$$[S] = \begin{bmatrix} \frac{1}{(1-\varpi_1)E_a} & \frac{-\nu_{ba}}{E_b} & \frac{-\nu_{ca}}{E_c} & 0 & 0 & 0 \\ \frac{-\nu_{ab}}{E_a} & \frac{1}{(1-\varpi_2)E_b} & \frac{-\nu_{cb}}{E_c} & 0 & 0 & 0 \\ \frac{-\nu_{ac}}{E_a} & \frac{-\nu_{bc}}{E_b} & \frac{1}{(1-\varpi_3)E_c} & 0 & 0 & 0 \\ 0 & 0 & 0 & \frac{1}{(1-\varpi_4)G_{ab}} & 0 & 0 \\ 0 & 0 & 0 & 0 & \frac{1}{(1-\varpi_5)G_{bc}} & 0 \\ 0 & 0 & 0 & 0 & 0 & \frac{1}{(1-\varpi_6)G_{ca}} \end{bmatrix} \quad (14)$$

The stiffness matrix $[C]$ is obtained by inverting the compliance matrix, i.e., $[C] = [S]^{-1}$. As suggested in Matzenmiller, et al., (1995), the growth rate of damage variables, ϖ_i , is governed by the damage rule of the form:

$$\dot{\varpi}_i = \max \{ \dot{\phi}_j q_{ij} \} \quad (15)$$

where the scalar damage functions $\dot{\phi}_j$ control the amount of growth and the vector-valued matrix q_{ij} ($i = 1, \dots, 6, j = 1, \dots, 13$) provide the coupling between the individual damage variables (i) and the various damage modes (j). Note that there are six damage modes ($j = 1, \dots, 6$) for the “unidirectional lamina model” and seven damage modes ($j = 7, \dots, 13$) for the “fabric lamina

model.” The damage criteria $f_j - r_j^2 = 0$ of Eqs. (1) to (12) provide the damage surfaces in strain space for the unidirectional and fabric lamina models, respectively. Damage growth, $\dot{\phi}_j > 0$, will occur when the strain path crosses the updated damage surface $f_j - r_j^2 = 0$ and the strain increment has a non-zero component in the direction of the normal to the damage surface, i.e., $\sum_i \frac{\partial f_j}{\partial \varepsilon_i} \dot{\varepsilon}_i > 0$. Combined with damage growth functions $\gamma_j(\varepsilon_i, \varpi_i)$; $\dot{\phi}_j$ is assumed to have the form:

$$\dot{\phi}_j = \sum_i \gamma_j \frac{\partial f_j}{\partial \varepsilon_i} \dot{\varepsilon}_i \quad (\text{no summation over } j) \quad (16)$$

Choosing

$$\gamma_j = \frac{1}{2} (1 - \phi_j) f_j^{\frac{m_j}{2} - 1} \quad (17)$$

and noting that

$$\sum_i \frac{\partial f_j}{\partial \varepsilon_i} \dot{\varepsilon}_i = \dot{f}_j \quad (18)$$

for the quadratic functions given by Eqs. (1) to (6) and Eqs. (8) to (12), lead to:

$$\dot{\phi}_j = \frac{1}{2} (1 - \phi_j) f_j^{\frac{m_j}{2} - 1} \dot{f}_j \quad (19)$$

where ϕ_j is the scalar damage function associated with the j^{th} failure mode, and m_j is a material constant for softening behavior. The scalar damage function ϕ_j can be obtained by integrating Eq. (19) as follows:

$$f_j = r_j^2 \rightarrow \begin{aligned} \dot{f}_j &= 2r_j \dot{r}_j \quad \& \\ f_j^{\frac{m_j}{2} - 1} &= r_j^{m_j - 2} \end{aligned} \quad (20)$$

$$\dot{\phi}_j = (1 - \phi_j) r_j^{m_j - 1} \dot{r}_j \rightarrow \int_0^{\phi_j} \frac{d\phi_j}{(1 - \phi_j)} = \int_0^{r_j} r_j^{m_j - 1} dr_j \dots \rightarrow \phi_j = 1 - \exp\left(\frac{1}{m_j} (1 - r_j^{m_j})\right)$$

The damage coupling matrix q_{ij} is considered for the unidirectional and fabric lamina models as follows.

DAMAGE COUPLING MATRIX FOR UNIDIRECTIONAL LAMINA MODEL

Eq. (21) is the damage coupling matrix, and Fig. 2 illustrates how Eq. (21) is associated with the modulus reduction for the unidirectional lamina model.

$$q_{ij}^U = \begin{bmatrix} 1 & 1 & 1 & 0 & 0 & 0 \\ 0 & 0 & 1 & 1 & 1 & 0 \\ 0 & 0 & 1 & 0 & 0 & 1 \\ 1 & 1 & 1 & 1 & 1 & 0 \\ 0 & 0 & 1 & 1 & 1 & 1 \\ 1 & 1 & 1 & 0 & 0 & 1 \end{bmatrix} \quad i = 1, \dots, 6; j = 1, \dots, 6. \quad (21)$$

UD DAMAGE TYPES		FIBER DAMAGE MODES			MATRIX DAMAGE MODES		
UD DAMAGE MODES		MODE 1u j = 1	MODE 2u j = 2	MODE 3u j = 3	MODE 4u j = 4	MODE 5u j = 5	MODE 6u j = 6
MODULI	q_{ij}^U						
E_a		1	1	1	0	0	0
E_b		0	0	1	1	1	0
E_c		0	0	1	0	0	1
G_{ab}		1	1	1	1	1	0
G_{bc}		0	0	1	1	1	1
G_{ca}		1	1	1	0	0	1

Figure 2: Coupling of Different Damage Modes to the Associated Reduction in Moduli for Unidirectional Lamina Model.

DAMAGE COUPLING MATRIX FOR FABRIC LAMINA MODEL

Eq. (22) is the damage coupling matrix, and Fig. 3 illustrates how Eq. (22) is associated with the modulus reduction for the fabric lamina model.

$$q_{ij}^F = \begin{bmatrix} 1 & 0 & 1 & 0 & 1 & 0 & 0 \\ 0 & 1 & 0 & 1 & 1 & 0 & 0 \\ 0 & 0 & 0 & 0 & 1 & 0 & 1 \\ 1 & 1 & 1 & 1 & 1 & 1 & 0 \\ 0 & 1 & 0 & 1 & 1 & 0 & 1 \\ 1 & 0 & 1 & 0 & 1 & 0 & 1 \end{bmatrix} \quad i = 1, \dots, 6; j = 7, \dots, 13. \quad (22)$$

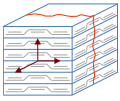
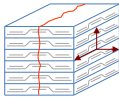
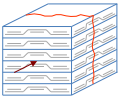
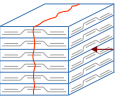
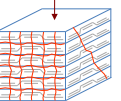
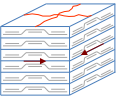
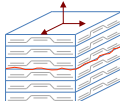
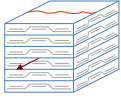
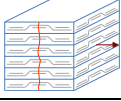
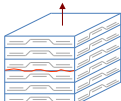
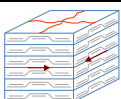
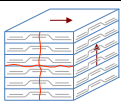
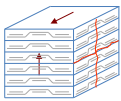
PW DAMAGE TYPES		FIBER DAMAGE MODES					MATRIX DAMAGE MODES	
PW DAMAGE MODES		MODE 1f j = 7	MODE 2f j = 8	MODE 3f j = 9	MODE 4f j = 10	MODE 5f j = 11	MODE 6f j = 12	MODE 7f j = 13
MO-DU-LI	q_{ij}^F							
E_a		1	0	1	0	1	0	0
E_b		0	1	0	1	1	0	0
E_c		0	0	0	0	1	0	1
G_{ab}		1	1	1	1	1	1	0
G_{bc}		0	1	0	1	1	0	1
G_{ca}		1	0	1	0	1	0	1

Figure 3: Coupling of Different Damage Modes to the Associated Reduction in Moduli for Fabric Lamina Model.

Through Eq. (15), the damage coupling matrix q_{ij} relates the individual damage variables ϖ_i to the various damage modes provided by the scalar damage functions ϕ_j for the unidirectional and fabric lamina models.

Unidirectional Fiber Modes 1u, 2u, & 3u: For the unidirectional lamina model, the damage coupling vectors q_{i1} and q_{i2} of equation (21) are chosen such that the fiber tension-shear and compressive damage modes 1u and 2u, Eqs. (1) & (2), provide the reduction of elastic moduli E_a , G_{ab} , and G_{ca} , due to ϖ_1 , ϖ_4 and ϖ_6 , respectively. The coupling vector q_{i3} provides that all the elastic moduli are reduced due to the fiber crush damage mode 3u, Eq. (3).

Unidirectional Matrix Modes 3u, 4u, & 5u: For the transverse matrix damage modes 4u and 5u, Eqs. (4) & (5), q_{i4} and q_{i5} provide the reduction of E_b , G_{ab} and G_{bc} , while for the through thickness matrix damage mode 6u, q_{i6} provides the reduction of E_c , G_{bc} , and G_{ca} .

Fabric Fiber Modes 1f, 2f, 3f, 4f, & 5f: For the fabric lamina model, the damage coupling vectors q_{i7} , q_{i8} , q_{i9} and q_{i10} are chosen for the fiber tension-shear and compressive damage modes 1f to 4f, Eqs. (8), & (9); such that the fiber damage in either the fill or warp direction results in stiffness reduction in the loading direction and in the related shear directions. For the fiber crush damage mode 5f, Eq (10), the damage coupling vector q_{i11} is chosen such that all the stiffness values are reduced as an element is failed under the crush mode.

Fabric Matrix Modes 6f, & 7f: For the in-plane matrix shear failure mode 6f given by Eq. (11), the stiffness reduction due to q_{i12} is limited to in-plane shear modulus, while the through thickness matrix damage (delamination) mode 7f, the coupling vector q_{i13} is chosen for the through thickness tensile modulus and transverse shear moduli.

NON-LINEAR PROGRESSIVE DAMAGE MODEL OF MAT162

Utilizing the damage coupling matrix given by Eqs. (21) & (22), and the scalar damage function given by Eq. (20), the damage variables ϖ_i can be obtained from Eq. (15) for an individual failure mode j as:

$$\varpi_i = 1 - \exp\left(\frac{1}{m_j}(1 - r_j^{m_j})\right), \rightarrow r_j \geq 1 \quad (23)$$

Note that the damage thresholds r_j given in the damage criteria of Eqs. (1) to (12) are continuously increasing functions with increasing damage. The damage thresholds have an initial value of one, which results in a zero value for the associated damage variable ϖ_i from Eq. (23). This provides an initial elastic region bounded by the damage functions in strain space. The nonlinear response is modeled by loading on the damage surfaces to cause damage growth with increasing damage thresholds and the values of damage variables ϖ_i . After damage initiated, the progressive damage model assumes linear elastic response within the part of strain space bounded by the updated damage thresholds. The elastic response is governed by the reduced stiffness matrix associated with the updated damage variables ϖ_i given in Eq. (14).

In defining the non-linear stress-strain behavior of a composite material in a specific direction k , a damage threshold r_k ($k = 1, \dots, 6$) can also be expressed as the ratio between the current total strain in the k^{th} direction and the corresponding yield strain.

$$r_k = \frac{\varepsilon_k}{\varepsilon_{ky}} \quad (24)$$

From Eq. 14, the Young's modulus in the k^{th} direction can now be expressed as:

$$E_k = (1 - \varpi_k) E_{k0} = E_{k0} \exp\left(\frac{1}{m_k} \left(1 - \frac{\varepsilon_k}{\varepsilon_{ky}}\right)^{m_k}\right) \quad (25)$$

Since the reduced modulus is also considered linear, the stress-strain relationship of the damaged material can now be expressed as:

$$\sigma_k = E_k \varepsilon_k = E_{k0} \varepsilon_k \exp\left(\frac{1}{m_k} \left(1 - \frac{\varepsilon_k}{\varepsilon_{ky}}\right)^{m_k}\right) \quad (26)$$

Recognizing the fact that $\sigma_{ky} = E_{k0} \varepsilon_{ky}$ Eq. (26) can also be expressed as:

$$\frac{\sigma_k}{\sigma_{ky}} = \frac{\varepsilon_k}{\varepsilon_{ky}} \exp\left(\frac{1}{m_k} \left(1 - \frac{\varepsilon_k}{\varepsilon_{ky}}\right)^{m_k}\right) \quad (27)$$

Fig. 4 shows the plot of Eq. (27) for different values of damage softening parameter, m . Note that the value of $r = \varepsilon / \varepsilon_y \leq 1$, represent the linear-elastic part of the stress-strain behavior, and Eq. (27) represents the post-yield damage softening behavior for $r = \varepsilon / \varepsilon_y \geq 1$.

It is well known that it is difficult to obtain the softening response of most quasi-brittle materials including fiber-reinforced composites. The softening response heavily depends on the set-up and test machines, which can lead to very scattered results. Consequently the choice of damage parameters for each mode becomes an open issue. Generally, smaller values of m make the material more ductile whereas higher values give the material more brittle behavior. A methodology to systematically determine the model material properties for penetration modeling has been successfully established in [Xiao et al., 2005].

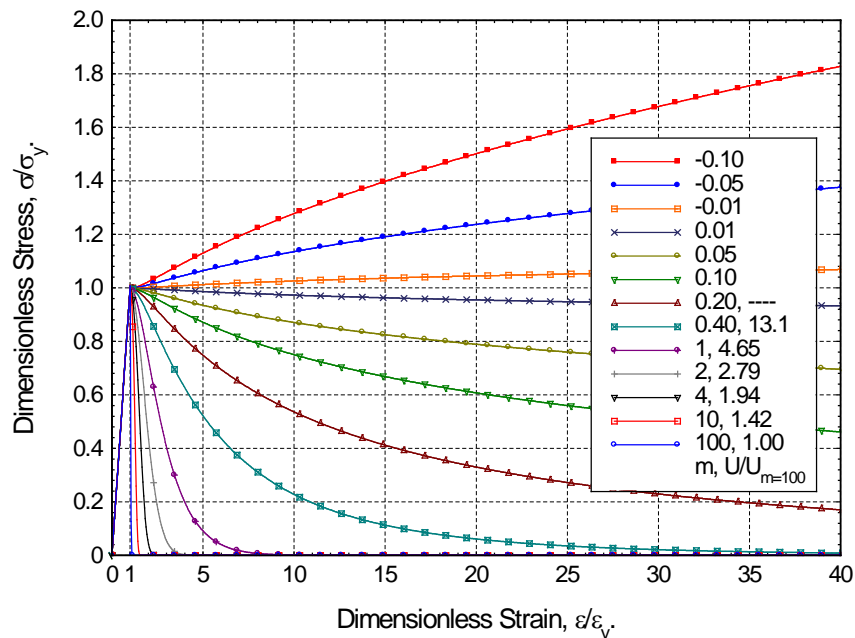


Figure 4: Non-Linear Progressive Damage Model of MAT162. Post-Yield Damage Softening of a Composite as a Function of Damage Softening Parameter m .

In MAT 162, the damage softening parameter m_1 controls the tensile and compressive fiber failure mode in a direction, and m_2 controls the transverse compressive matrix failure mode in b direction for the “unidirectional lamina model.” However, for fabric the “fabric lamina model,” m_2 controls the softening of tensile and compressive fiber failure mode in b direction. m_3 is for softening related to fiber crush mode, and m_4 is for both perpendicular and parallel matrix mode for “unidirectional” case, and for both in-plane matrix failure and through the thickness matrix failure for “fabric” case. Detail analysis on m parameters on the stress-strain behavior can be found in Ref. [Gama et al., 2009].

ADDITIONAL DISCUSSION ON MODULI AND STRENGTH REDUCTION

When fiber tension-shear damage is predicted in a layer by equation (1) or (8), the load carrying capacity of that layer in the associated direction is reduced to zero according to damage variable Eq. (23). For compressive fiber damage due to equation (2) or (9), the layer is assumed to carry a residual axial load in the damaged direction. The damage variables of Eq. (23) for the compressive modes have been modified to account for the residual strengths of $S_{aCR} = S_{aC} \times S_{FFC}$ and $S_{bCR} = S_{bC} \times S_{FFC}$ in the fill and warp directions, respectively.

For through thickness matrix (delamination) failure given by equation (6) or (12), the in-plane load carrying capacity within the element is assumed to be elastic (i.e., no in-plane damage). The load carrying behavior in the through thickness direction is assumed to depend on the opening or closing of the matrix damage surface. For tensile mode, $\epsilon_c > 0$, the through thickness stress components are softened and reduced to zero due to the damage criteria described above.

For compressive mode, $\varepsilon_c < 0$, the damage surface is considered to be closed, and thus, ε_c is assumed to be elastic, while ε_{bc} and ε_{ca} are allowed to reduce to sliding friction traction of equation (7) or (13). Accordingly, for the through thickness matrix failure under compressive mode, the damage variable equation is further modified such that the residual sliding strength value is equal to S_{SRC} .

EFFECT OF STRAIN RATES ON STRENGTH AND MODULI

The effect of strain-rate on the nonlinear stress-strain response of a composite layer is modeled by a logarithmic strain-rate dependent function for the moduli and strength of the form:

$$\frac{X_{RT}}{X_0} = 1 + C_{rate} \ln \left(\frac{\dot{\varepsilon}}{\dot{\varepsilon}_0} \right) \quad (28)$$

where, X_{RT} is the rate dependent property of interest at an average strain rate of $\dot{\varepsilon}$, and X_0 is the quasi-static property of interest at an average reference strain rate of $\dot{\varepsilon}_0$. In the present MAT162 formulation, the reference strain rate is chosen to be:

$$\dot{\varepsilon}_0 = 1 \text{ s}^{-1} \quad (29)$$

This implies, that the unit of time in LS-DYNA® MAT162 analysis has to be second (s). If millisecond (ms) or microsecond (us) time units are used, the rate effects will not be effective!

EFFECT OF STRAIN RATE ON STRENGTH PROPERTIES

One average rate parameter, CERATE1 or C_{rate1} is used to add rate effects on strength properties as follows:

$$\{S_{RT}\} = \{S_0\} \left(1 + C_{rate1} \ln \left(\frac{\left\{ \frac{\dot{\varepsilon}}{\dot{\varepsilon}_0} \right\}}{\dot{\varepsilon}_0} \right) \right) \quad (30)$$

where, the strength and strain rate matrices are given by Eq. (31). Note that the through thickness tensile strength S_{cT} , and the shear strengths S_{ab} , S_{bc} , & S_{ca} ; are not considered as rate dependent in MAT162 formulation.

EFFECT OF STRAIN RATE ON MODULI

Three rate parameters, C_{rate2} , C_{rate3} , & C_{rate4} are used to add rate effects on three axial and three shear moduli as presented in Eq. (32), where, the moduli, strain rate, and rate parameter matrices

are given by Eq. (33). Note that the rate effects on both the axial moduli, E_a & E_b , are controlled by the rate parameter C_{rate2} , and that for the through thickness modulus, E_c , by C_{rate4} . In addition, the rate effects on the shear moduli, G_{ab} , G_{bc} , & G_{ca} , are controlled by the rate parameter C_{rate3} .

$$\{S\} = \begin{Bmatrix} S_{aT} \\ S_{aC} \\ S_{bT} \\ S_{bC} \\ S_{FC} \\ S_{FS} \end{Bmatrix}, \& \{\dot{\epsilon}\} = \begin{Bmatrix} |\dot{\epsilon}_a| \\ |\dot{\epsilon}_a| \\ |\dot{\epsilon}_b| \\ |\dot{\epsilon}_b| \\ |\dot{\epsilon}_c| \\ (\dot{\epsilon}_{ca}^2 + \dot{\epsilon}_{bc}^2)^{1/2} \end{Bmatrix} \quad (31)$$

$$\{E_{RT}\} = \{E_0\} \left(1 + \{C_{rate}\} \ln \frac{\{\dot{\epsilon}\}}{\dot{\epsilon}_0} \right) \quad (32)$$

$$\{E_{RT}\} = \begin{Bmatrix} E_a \\ E_b \\ E_c \\ G_{ab} \\ G_{bc} \\ G_{ca} \end{Bmatrix}, \{\dot{\epsilon}\} = \begin{Bmatrix} |\dot{\epsilon}_a| \\ |\dot{\epsilon}_b| \\ |\dot{\epsilon}_c| \\ |\dot{\epsilon}_{ab}| \\ |\dot{\epsilon}_{bc}| \\ |\dot{\epsilon}_{ca}| \end{Bmatrix}, \& \{C_{rate}\} = \begin{Bmatrix} C_{rate2} \\ C_{rate2} \\ C_{rate4} \\ C_{rate3} \\ C_{rate3} \\ C_{rate3} \end{Bmatrix} \quad (33)$$

A discussion of rate dependent MAT162 properties can be found in Ref. [Gama & Gillespie Jr. 2011].

ELEMENT EROSION

A failed element is eroded in any of three different ways:

1. If fiber tensile failure in a “unidirectional” layer is predicted in the element and the axial tensile strain is greater than E_LIMIT. For a “fabric” layer, both in-plane directions are failed and exceed E_LIMIT.
2. If compressive relative volume (ratio of current volume to initial volume) in a failed element is smaller than ECRSH.
3. If expansive relative volume in a failed element is greater than EEXPN.

FINITE ELEMENT MODELING TIPS

- One point integration solid element (TYPE = 1) can be used for MAT162.
- In order to observe the delamination at the interface between two adjacent laminae, two different PART IDs with different MAT IDs for each part and with different material orientation angles (BETA in the MAT162 cards) must be defined at the interface of interest. If it is required to model the delamination at the interface between two plies with the same material orientation angles, those two angles must be defined in different ways in each PART, e.g., BETA = 0.00 & BETA = 180.00.
- *DATABASE_EXTENT_BINARY must be included to check history variables.
- Type of *HOURLASS need to be checked for minimum hourglass energy over the duration of the LS-DYNA solution.

DAMAGE HISTORY PARAMETERS

Information about the damage history variables for the associated failure modes can be plotted in LS-POST. These additional variables are tabulated below:

History Variable			Description	Value	LS-POST Components
#	Uni	Fabric			
1	$\max(r_1, r_2)$	$\text{Max}(r_7, r_9)$	Fiber mode in a	0 - elastic > 1- damage thresholds, Eqs. (1-6) to (8-12)	7
2	-	$\text{Max}(r_8, r_{10})$	Fiber mode in b		8
3	r_3	r_{11}	Fiber crush mode		9
4	r_5	r_{12}	Perpendicular matrix mode		10
5	r_6	r_{13}	Parallel matrix/ delamination mode		11
6			Element delamination indicator	0 – no delamination 1 – with delamination	12

REFERENCES







- Yen, C.F., (2002), "Ballistic Impact Modeling of Composite Materials," Proceedings of 7th International LS-DYNA Users Conference, May, 2002, Dearborn, Michigan, pp.6.15-6.26.
- Matzenmiller, A., Lubliner, J., and Taylor, R.L. (1995). "A Constitutive Model for Anisotropic Damage in Fiber-Composites," *Mechanics of Materials*, 20, pp. 125-152.
- Xiao, J. R., Gama, B. A., and Gillespie Jr., J. W., "Progressive Damage and Delamination in Plain Weave S-2 Glass/SC-15 Composites under Quasi-Static Punch Shear Loading," *Composite Structures*, 2007, Vol. 78, pp. 182-196.
- Gama, B. A., Travis A. Bogetti, and Gillespie, J. W. (1009). "Progressive Damage Modeling of Plain-Weave Composites using LS-Dyna Composite Damage Model MAT162," Proceedings and CD Rom of 7th European LS-DYNA Conference, May 14-15, Salzburg, Austria, 2009.
- Gama, B. A., and Gillespie, J. W. (2011). "Finite Element Modeling of Impact, Damage and Penetration of Thick-Section Composites," *International Journal of Impact Engineering*, Vol. 38, pp. 181-197.
- Bazle Z. (Gama) Haque, Jessica L. Harrington, Ishita Biswas, and John W. Gillespie Jr. "Perforation and Penetration of Composites." CD Proceedings, SAMPE 2012 Baltimore, MD. May 21-24, 2012.
- Bazle Z. (Gama) Haque, Jessica L. Harrington, and John W. Gillespie Jr. "Multi-hit ballistic impact on S-2 glass/SC15 thick-section composites: Finite element analyses." *Journal of Strain Analysis*, Vol. 47, No. 7, 2012. DOI: 10.1177/0309324712456823.
- Bazle Z. (Gama) Haque, Richard J. Stanton, and John W. Gillespie Jr. "Perforation Mechanics of Thin Composites." CD Proceedings, SAMPE 2013 Long Beach, CA. May 6-9, 2013.
- Jordan, J. B., Naito, C. J., and (Gama) Haque, B. Z. Progressive damage modeling of plain weave E-glass/phenolic composites. *Composites B*, Vol. 61, May 2014, pp. 315-323.

APPENDIX A: MAT162 PROPERTIES AND PARAMETERS

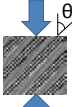
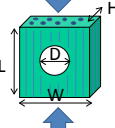
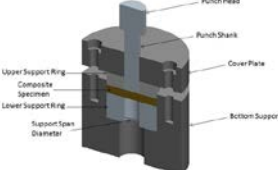
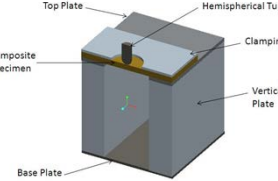
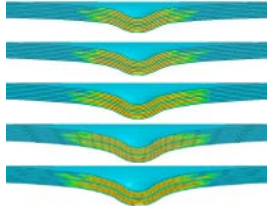
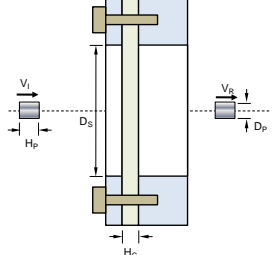
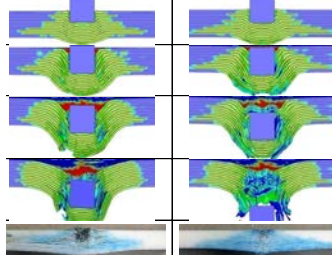
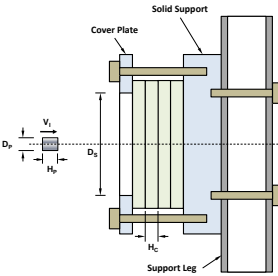
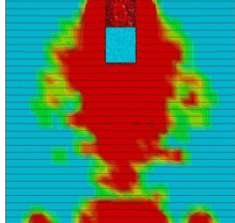
MAT162 ELASTIC AND STRENGTH PROPERTIES

In addition to ASTM standard test methods, UD-CCM has developed non-standard experimental techniques and computational methodologies to determine all material properties and parameters needed for MAT162.

MAT162 ELASTIC & STRENGTH PROPERTIES: ASTM STANDARD TESTS

Properties, Parameters	Test Method	Specimen	Dimensions (mm)	Miscellaneous
E_1, ν_{12}, X_1^T	0° Tension (ASTM D3039)		254×25.4×1	
E_2, ν_{21}, X_2^T	90° Tension (ASTM D3039)		175×25.4×2	
X_1^C	0° Compression (ASTM D3410)		155×25.4×2	
X_2^C	90° Compression (ASTM D3410)		155×25.4×2	
$E_2, \nu_{31}, \nu_{32}, X_3^T$	Thru-thickness Tension (no standard)		20×20×20	
G_{12}, G_{23}, G_{31} S_{12}, S_{23}, S_{31}	In-Plane +/-45 Tension, Rail-Shear & V-Notch Shear (ASTM D5379)		76×4.5×20	Shear in 1-2, 2-3, 3-1 planes

**MAT162 PROPERTIES & PARAMETERS:
NON-STANDARD UD-CCM TEST & COMPUTATIONAL METHODOLOGIES**

<p>$E_3, PHIC$</p>	<p>Out-of-Plane Off-Axis Compression (no standard)</p>		<p>15x15x15</p>	<p>$\theta = 0^\circ, 15^\circ, 30^\circ, 45^\circ, 60^\circ, 75^\circ$</p>
<p>$SFFC$</p>	<p>Open Hole Compact Compression Test (no standard)</p>		<p>25x25x13 D = 8~12</p>	<p>Loading along fiber direction for both UD and PW Composites</p>
<p>SFC, SFS</p>	<p>Quasi-Static Punch Shear Test (QS-PST) Punch Crush Strength (PCS) & Punch Shear Strength (PSS) (BZH Methodology)</p>		<p>25 mm Discs 100x100 Plates 150x150 Plates</p>	<p>$SPR = D_s/D_p$ $SPR = 0$ for SFC $SPR = 1.1$ for SFS</p>
<p>$OMGMX$ & Damage Softening Parameters m_1 to m_4</p>	<p>Low Velocity Impact Experiments; & Numerical Simulation (BZH Methodology)</p>		<p>100x150 Plates</p>	 <p>Energy Levels: 30J to 70J @ an increment of 10J</p>
<p>Erosion Parameters E_{LIMT} E_{EXP} Rate Parameters C_{rate1} to C_{rate4}</p>	<p>Hopkinson Bar Testing Dynamic Punch Shear Ballistic Testing Numerical Simulation of Ballistic Tests (BZH Methodology)</p>		<p>150x150x15 Plates</p>	
<p>Crush Parameters $SFC, ECRSH$</p>	<p>Depth of Penetration Impact Experiments; & Numerical Simulation (BZH Methodology)</p>		<p>305x205x50 Plates</p>	 <p>Impact at 300 to 800 m/s @ an interval of 50 m/s. Measure DoP as a function of impact velocity. Parametrically determine SFC & ECRSH to match the Experimental Data.</p>

MAT162 DATABASE OF COMPOSITE PROPERTIES

Properties, Unit	UD S-2 Glass/SC15	PW S-2 Glass/SC15	PW S-Glass/Phenolic OWENS Corning	PW E-Glass/Phenolic U.S. AERDC
V _f	0.60	0.53	0.62	0.66
ρ_C , g/cm ³	1.85	1.85	2.00	2.107
E1, GPa	64.0	27.5	38.6	29.15
E2, GPa	11.8	27.5	31.9	29.15
E3, GPa	11.8	11.8	12.0	11.00
v ₂₁	0.0535	0.110	0.100	0.078
v ₃₁	0.0535	0.180	0.200	0.109
v ₃₂	0.449	0.180	0.200	0.109
G12, GPa	4.30	2.90	4.50	1.54
G23, GPa	3.70	2.14	2.90	1.67
G31, GPa	4.30	2.14	3.10	1.67
X1T, MPa	1380	604	402	531
X1C, MPa	770	291	138	131
X2T, MPa	47	604	592	531
X2C, MPa	137	291	204	131
X3T, MPa	47	58	52	50
SFC, MPa	850	850	1540	870
SFS, Mpa	250	300	172	160
S12, MPa	76	75	73	35
S23, MPa	38	58	49	27
S31, MPa	76	58	49	27
AM1	100.00	2.00	1.00	1.00
AM2	10.00	2.00	1.00	1.00
AM3	1.00	0.50	0.50	0.50
AM4	0.10	0.20	-0.20	0.20/-0.20
PHIC	10	10	10	10
SFFC	0.10	0.30	0.30	0.30
Crate1	0.00	0.03	0.03	0.03
Crate2	0.00	0.00	0.00	0.00
Crate3	0.00	0.03	0.03	0.03
Crate4	0.00	0.03	0.03	0.03
SDELM	1.2	1.2	1.2	1.2
OMGMX	0.999	0.999	0.998 (LVI) 0.997 (DoP)	0.994
E_LIMT	4.5	4.5	5.0	4.0
EEXPN	4.5	4.5	5.0	4.0
ECRSH	0.001	0.001	0.700	0.500
AMODEL	1 (UD)	2 (PW)	2 (PW)	2 (PW)
SOURCE	Ref. [A]	Ref. [B]	Ref. [C]	Ref. [D]

REFERENCES

- [A]. Kang, S-K., Gama, B. A., and Gillespie, Jr., J. W. SAMPE 2010.
[B]. Gama, B. A., and Gillespie, Jr., J. W. 11th European LS-Dyna Conference, 2009.
[C]. (Gama) Haque, B. Z., Hartman, D. R., et al. SAMPE 2011, ASC 2012.
[D]. Jordan, J., & (Gama) Haque, B. Z., et al. Technical Report, 2012.

APPENDIX B: GENERAL DISCUSSION

DISCUSSION ON REFERENCE STRAIN RATE

The reference strain rate in MAT162 is set to 1. If the time unit in LS-DYNA computation is set to seconds (s), then this reference strain rate is $\dot{\epsilon}_0 = 1s^{-1}$. This raises a question of how to calculate the rate parameters, C_{rate} , for different time units of LS-DYNA computations.

Consider a fictitious experimental set of strength data as a function of strain rates measured in s^{-1} . Table SR-1 shows this set of data. Fig. SR-1a shows the plot of this set of experimental data. The MAT162 rate equation is expressed as:

$$\frac{X_{RT}}{X_0} = 1 + C_{rate} \ln\left(\frac{\dot{\epsilon}}{\dot{\epsilon}_0}\right) \quad (\text{SR-1})$$

Table SR-1: A Fictitious Experimental Set of Strength Data and Dimensionless Data for Reference Strain Rate, $\dot{\epsilon}_0 = 1.0 \times 10^{-6} s^{-1}$.

Strain Rate, s^{-1}	Strength, MPa	$\dot{\epsilon}_0 = 1.0 \times 10^{-6} s^{-1}$	$X_0 = 600 MPa$
$\dot{\epsilon}$	X_{RT}	$\dot{\epsilon}/\dot{\epsilon}_0$	X_{RT}/X_0
1.00E-06	600	1.00E+00	1.0000
1.00E-05	630	1.00E+01	1.0500
1.00E-04	655	1.00E+02	1.0917
1.00E-03	680	1.00E+03	1.1333
1.00E-02	710	1.00E+04	1.1833
1.00E-01	740	1.00E+05	1.2333
1.00E+00	765	1.00E+06	1.2750
1.00E+01	790	1.00E+07	1.3167
1.00E+02	820	1.00E+08	1.3667
1.00E+03	850	1.00E+09	1.4167
1.00E+04	875	1.00E+10	1.4583

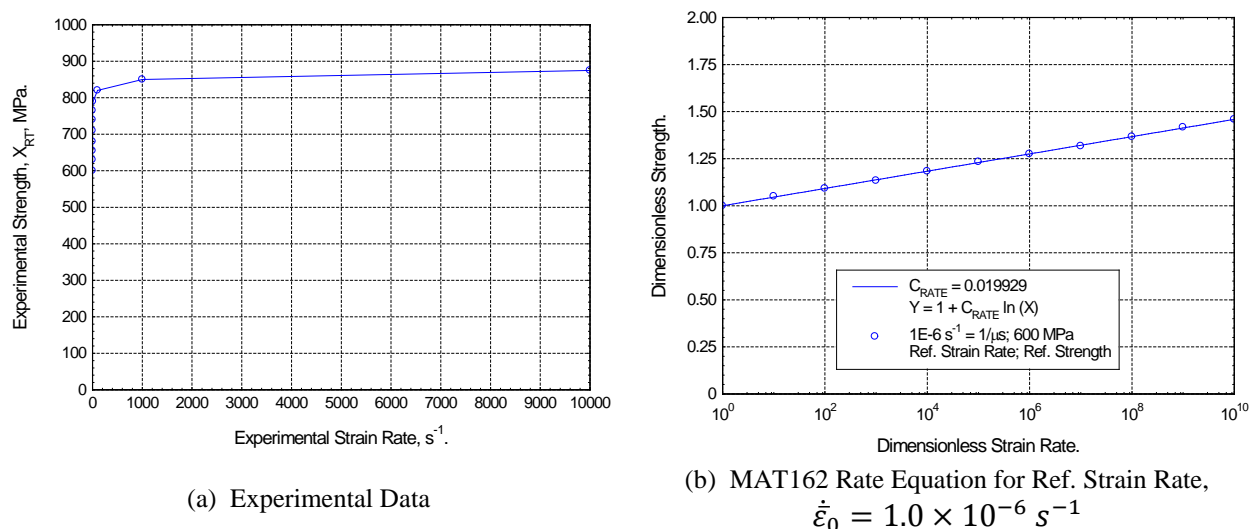


Figure SR-1: A Fictitious Experimental Set of Strength MAT162 Rate Equation for Reference Strain Rate, $\dot{\epsilon}_0 = 1.0 \times 10^{-6} s^{-1}$.

We will use the Table SR-1 data to determine the rate parameter for different time units in LS-DYNA computations.

1. Reference Strain Rate $\dot{\epsilon}_0 = 1.0 \times 10^{-6} s^{-1} = 1/\mu s$ for LS-DYNA Time Unit of Micro-Second

Consider the LS-DYNA time unit be micro-second. Also consider the reference strain rate in micro-second time unit to be $\dot{\epsilon}_0 = 1 \mu s^{-1} = 1.0 \times 10^{-6} s^{-1}$. From Table SR-1, the reference strength is $X_0 = 600 MPa$. We can then normalize the experimental data with the reference strain rate and reference strength and the dimensionless values ($\dot{\epsilon}/\dot{\epsilon}_0, X_{RT}/X_0$) are also presented in Table SR-1. The dimensionless strength and strain rates can then be plotted and is presented in Fig. SR-1b. Eq. (SR-1) can then be used to fit the dimensionless experimental data in determining the rate parameter, C_{rate} , and for the fictitious experimental data presented in Table SR-1 is found to be, $[C_{rate}]_{\dot{\epsilon}_0=1 \mu s^{-1}} = 0.019929$.

2. Reference Strain Rate $\dot{\epsilon}_0 = 1.0 \times 10^{-3} s^{-1} = 1/ms$ for LS-DYNA Time Unit of Milli-Second

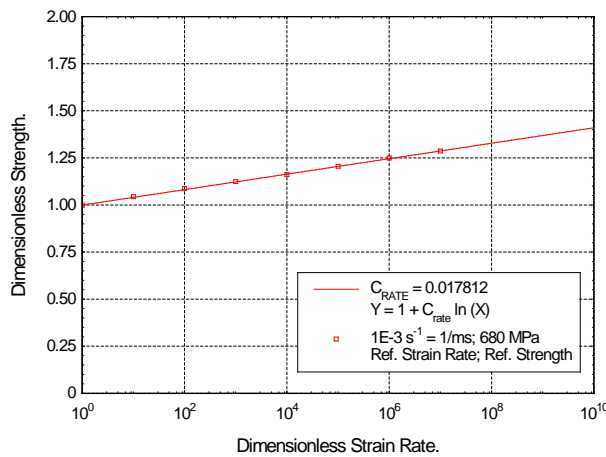
Consider the LS-DYNA time unit be milli-second. Also consider the reference strain rate in milli-second time unit to be $\dot{\epsilon}_0 = 1 ms^{-1} = 1.0 \times 10^{-3} s^{-1}$. The corresponding reference strength is $X_0 = 680 MPa$. Table SR-2 shows the dimensionless strain rate and stress data and is plotted in Fig. SR-2a. Note that strain rates $< 1.0 \times 10^{-3} s^{-1}$ are not considered. This data is curve fitted to determine the rate parameter and is found to be, $[C_{rate}]_{\dot{\epsilon}_0=1 ms^{-1}} = 0.017812$.

Table SR-2: A Fictitious Experimental Set of Strength Data and Dimensionless Data for Reference Strain Rate, $\dot{\epsilon}_0 = 1.0 \times 10^{-3} s^{-1}$, and $\dot{\epsilon}_0 = 1.0 s^{-1}$.

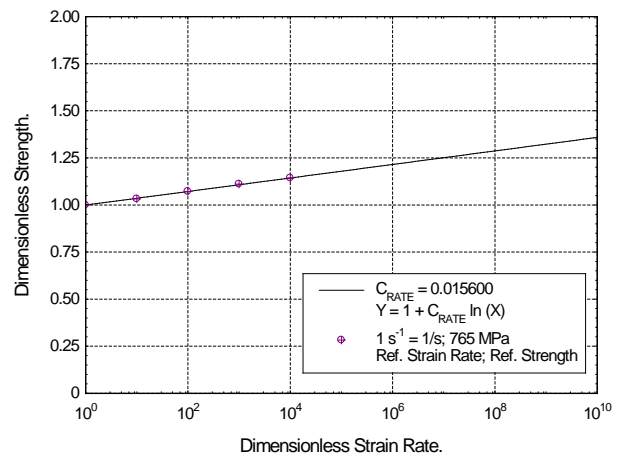
Strain Rate, s^{-1}	Strength, MPa	$\dot{\epsilon}_0 = 1.0 \times 10^{-3} s^{-1}$	$X_0 = 680 MPa$	$\dot{\epsilon}_0 = 1.0 s^{-1}$	$X_0 = 765 MPa$
$\dot{\epsilon}$	X_{RT}	$\dot{\epsilon}/\dot{\epsilon}_0$	X_{RT}/X_0	$\dot{\epsilon}/\dot{\epsilon}_0$	X_{RT}/X_0
1.00E-06	600	-	-	-	-
1.00E-05	630	-	-	-	-
1.00E-04	655	-	-	-	-
1.00E-03	680	1.00E+00	1.0000	-	-
1.00E-02	710	1.00E+01	1.0441	-	-
1.00E-01	740	1.00E+02	1.0882	-	-
1.00E+00	765	1.00E+03	1.1250	1.00E+00	1.0000
1.00E+01	790	1.00E+04	1.1618	1.00E+01	1.0327
1.00E+02	820	1.00E+05	1.2059	1.00E+02	1.0719
1.00E+03	850	1.00E+06	1.2500	1.00E+03	1.1111
1.00E+04	875	1.00E+07	1.2868	1.00E+04	1.1438

3. Reference Strain Rate $\dot{\epsilon}_0 = 1.0 s^{-1} = 1/s$ for LS-DYNA Time Unit of Second

Consider the LS-DYNA time unit be second. Also consider the reference strain rate in second time unit to be $\dot{\epsilon}_0 = 1 s^{-1}$. The corresponding reference strength is $X_0 = 765 MPa$. Table SR-2 shows the dimensionless strain rate and stress data and is plotted in Fig. SR-2b. Note that strain rates $< 1.0 s^{-1}$ are not considered. This data is curve fitted to determine the rate parameter and is found to be, $[C_{rate}]_{\dot{\epsilon}_0=1 ms^{-1}} = 0.015600$.



(a) MAT162 Rate Equation for Ref. Strain Rate, $\dot{\epsilon}_0 = 1.0 \times 10^{-3} s^{-1}$



(b) MAT162 Rate Equation for Ref. Strain Rate, $\dot{\epsilon}_0 = 1.0 s^{-1}$

Figure SR-2: MAT162 Rate Equations for Reference Strain Rates, $\dot{\epsilon}_0 = 1.0 \times 10^{-3} s^{-1}$, and $\dot{\epsilon}_0 = 1.0 s^{-1}$.

DISCUSSION ON LAMIANTE ARCHITECTURE AND PREDEFINED DELAMINATION PLANES

A composite laminate may contain several numbers of laminas or plies stacked through-the-thickness of the laminate. If the individual laminas are very thin, it is suggested to combine several laminas into one sub-laminate. Figure LA-1 shows the finite element model of such a sub-laminate with three (3) through-thickness elements.

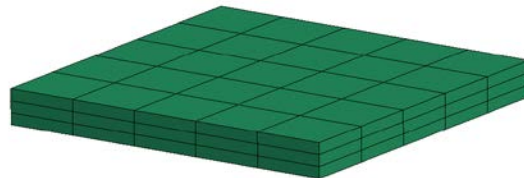


Figure LA-1: Finite Element Model of a Sub-Laminate with Three (3) Through-Thickness Elements.

Once a sub-laminate model is created, one should assign a Part ID to the sub-laminate and associate the **PID** with a Material ID with a pre-defined material angle (**BETA**), e.g.; **PID=1, MID=100, BETA=0** in Fig. LA-2. Several sub-laminates can be stacked through-the-thickness to build a laminate. Figure LA-2 shows a composite laminate with four (4) sub-laminates stacked through-the-thickness with the stacking sequence [0/90/0/90] and each sub-laminates are assigned with different Part IDs, i.e., **PID=1, 2, 3, 4**. However, since the stacking sequence is taken as [0/90/0/90], only two Material IDs (i.e., **MID=100, 200**) are sufficient. Note that all duplicate nodes between the PIDs 1 to 4 needs to be merged and the unreferenced nodes be deleted.

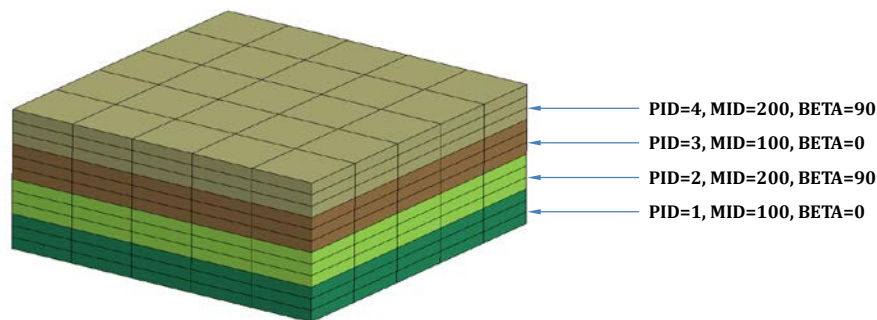


Figure LA-2: Node Merged Finite Element Model of a Laminate consisting of Four (4) Sub-Laminates with the Stacking Sequence [0/90/0/90]. Three Delamination Planes are thus Predefined between PIDs 1&2, 2&3, and 3&4.

According to MAT162 formulations, three pre-defined delamination planes will be automatically defined at the interface between four parts with different material angles (**BETA**). Once delamination between two parts with different material angles is predicted, shear properties of the elements adjacent to the delamination interface will be degraded to mimic delamination without creating physical surfaces between sub-laminates or parts. The advantage of MAT162

delamination criterion is that it is simple, however, the disadvantage is that the predicted delamination is assigned a thickness equal to one element near the delamination interface and is not physical in nature. This is why, three elements through-the-thickness of a sub-laminate or part is proposed so that the pseudo-delamination is limited to one-third of the thickness of a sub-laminate or part.

Figures LA-3 to 5 show three additional laminate stacking sequences defined with four sub-laminates.

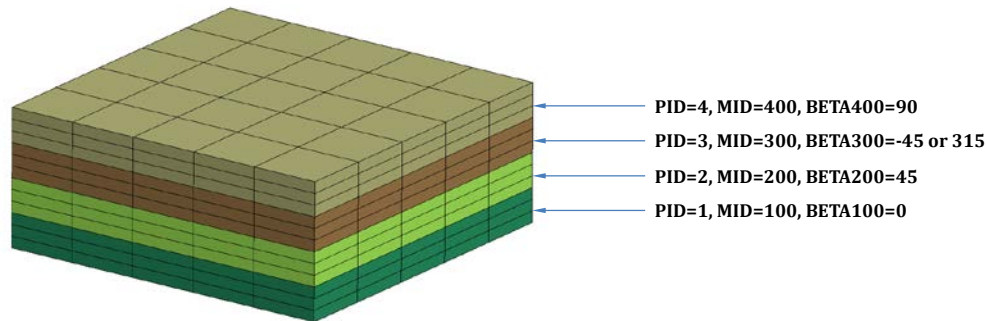


Figure LA-3: Node Merged Finite Element Model of a Laminate consisting of Four (4) Sub-Laminates with the Stacking Sequence [0/45/-45/90]. Three Delamination Planes are thus Predefined between PIDs 1&2, 2&3, and 3&4.

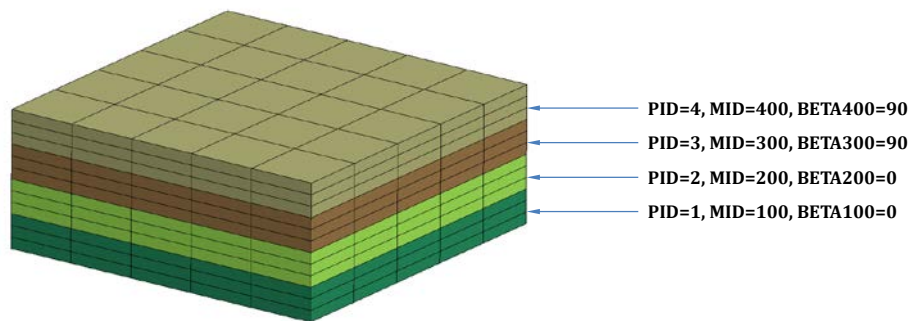


Figure LA-4: Node Merged Finite Element Model of a Laminate consisting of Four (4) Sub-Laminates with the Stacking Sequence [0/0/90/90]. One Delamination Plane is thus Predefined between PIDs 2&3.

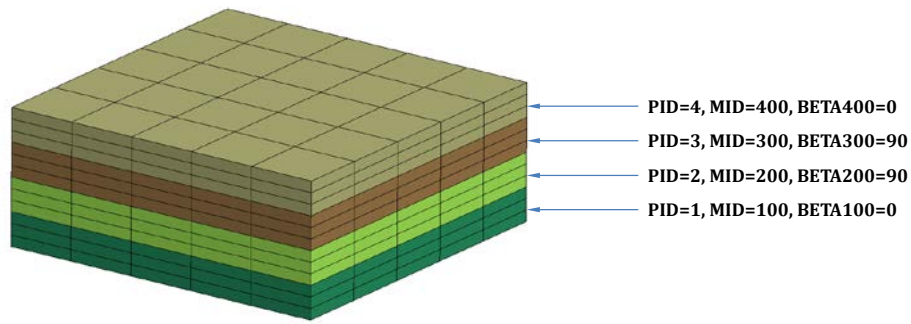


Figure LA-5: Node Merged Finite Element Model of a Laminate consisting of Four (4) Sub-Laminates with the Stacking Sequence [0/90/90/0]. Two Delamination Planes are thus Predefined between PIDs 1&2, and 3&4.

DISCUSSION ON CONTROL ACCURACY

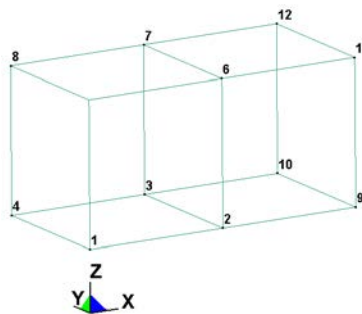


Figure CA-1: Definition of Two Single Elements in the Discussion of Control Accuracy.

In Fig. CA-1, if we choose **AOPT=0** for a composite element and define the element (**EID=1**) with the following node sequence, then the vector **V12** connecting nodes 1 & 2 defines the material direction 1 or A. The vector **V14** connecting nodes 1 & 4 together with the vector **V12** defines the material plane 1-2 or A-B, and the vector cross product **V12 × V14** defines the through-thickness material direction 3 or C.

```

$-----+-----+-----+-----+-----+-----+-----+-----+
*ELEMENT_SOLID
$-----+-----+-----+-----+-----+-----+-----+-----+
$#   eid   pid   n1    n2    n3    n4    n5    n6    n7    n8
$-----+-----+-----+-----+-----+-----+-----+-----+
      1    100    1     2     3     4     5     6     7     8
$-----+-----+-----+-----+-----+-----+-----+-----+
    
```

Following the same procedure, one can define the second element (**EID=2**) as follows to be consistent with **AOPT=0**.

```

$-----+-----+-----+-----+-----+-----+-----+-----+-----+
*ELEMENT_SOLID
$-----+-----+-----+-----+-----+-----+-----+-----+-----+
$#  eid      pid      n1      n2      n3      n4      n5      n6      n7      n8
$-----+-----+-----+-----+-----+-----+-----+-----+-----+
      2      100      9      10      3      2      11      12      7      6
$-----+-----+-----+-----+-----+-----+-----+-----+-----+
    
```

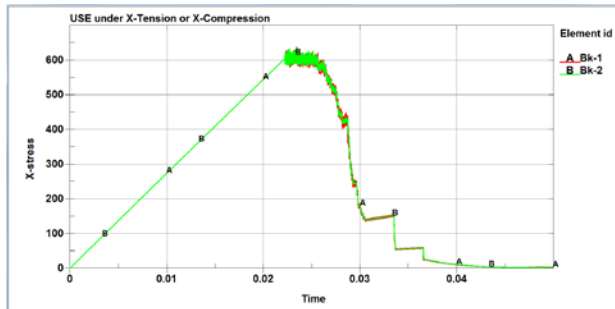
However, if the second element (**EID=2**) is defined as follows, then it is not consistent with **AOPT=0**.

```

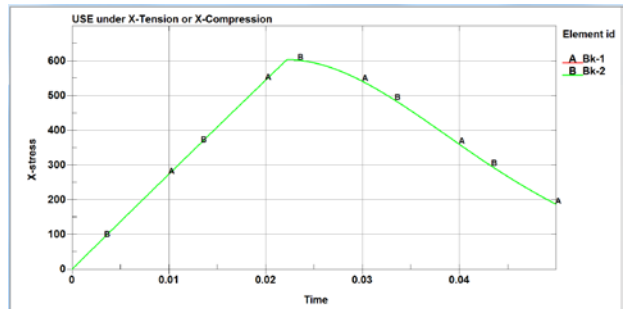
$-----+-----+-----+-----+-----+-----+-----+-----+-----+
*ELEMENT_SOLID
$-----+-----+-----+-----+-----+-----+-----+-----+-----+
$#  eid      pid      n1      n2      n3      n4      n5      n6      n7      n8
$-----+-----+-----+-----+-----+-----+-----+-----+-----+
      1      100      1      2      3      4      5      6      7      8
      2      100      2      9      10     3      6      11     12     7
$-----+-----+-----+-----+-----+-----+-----+-----+-----+
    
```

One can try to fix this problem by choosing **AOPT=2** by defining two vectors **A**(1, 0, 0) & **B**(0, 1, 0) to represent material direction 1 or A and the plane 1-2 or A-B, but this will not correct the problem, instead produce a wrong material response.

Figure CA-2a shows the wrong stress-time plot using **AOPT=2** with the wrong element definition for **EID=2**. In order to solve this problem, the LS-DYNA control card ***CONTROL_ACCURACY** can be used which allows **INVARIANT NODE NUMBERING** if the parameter **INN=3** is chosen for solid elements. Figure CA-2b shows the correct stress-time response with **INN=3** in the control accuracy card.



(a) AOPT=2 with INN=1



(a) AOPT=2 with INN=3

Figure CA-2: Definition of Two Single Elements in the Discussion of Control Accuracy.

EXAMPLE OF *CONTROL_ACCURACY CARD WITH PARAMETERS

```

$-----+-----+-----+-----+-----+-----+-----+
*PARAMETER_EXPRESSION
$-----+-----+-----+-----+-----+-----+-----+
$ PRMR1  EXPRESSION1
$-----+-----+-----+-----+-----+-----+-----+
I INN    3
$-----+-----+-----+-----+-----+-----+-----+
...
...
...
...
...
$-----+-----+-----+-----+-----+-----+-----+
*CONTROL_ACCURACY
$-----+-----+-----+-----+-----+-----+-----+
$#      osu      inn  pidosu
        0        &INN
$-----+-----+-----+-----+-----+-----+-----+

```

AXIS OPTION AOPT AND SWITCHING MATERIAL AXES

Axis options, **AOPT=0, 2, 4** has been tested and are found to be working with MAT162 along with the material axes switch options **MACF** without any problems. At present, we are looking at the applicability of axis option **AOPT=1**, and will report when our test is complete.

This Page is Intentionally Left Blank